ter constrain the locking depth and rupture potential of the Hayward fault (Figure 10.17). The figure shows results from joint inversions of both the InSAR and GPS data for slip rate on the creeping Hayward fault. We find that the current GPS data set provides little added constraint to the shallow slip on the Hayward fault. However, the GPS data allow us an improved representation and integration of the deeply seated regional strain accumulation. The initial inversions of the two data sets suggests a creep depth of 7 km is favored by the 1992-1997 InSAR data and current GPS data set (Figure 10.18). We are currently in the process of establishing a denser GPS network in this area with sites chosen to optimize our resolution of slip potential on the northern Hayward fault. The L1 system developed at UNAVCO is currently being tested at BSL to aid us in this effort. InSAR geodesy promises to be an extremely valuable tool to resolve highly detailed images of subsurface slip and elastic strain accumulation.

8.3 References

Bürgmann, R., E. Fielding, and J. Sukhatme, Slip along the Hayward fault, California, estimated from space-based synthetic aperture radar interferometry. *Geology, 26,* 559-562, 1998.

Lienkaemper, J.J., J.S. Galehouse, and R.W. Simpson, Creep response of the Hayward fault to stress changes caused by the Loma Prieta earthquake, *Science, 276,* 2014-2016, 1997.

Toppozada, T.R., and G. Borchardt, Re-evaluation of the 1836 "Hayward fault" and the the 1838 San Andreas fault earthquakes, *Bull. Seismol. Soc. Am., 88,* 140-159, 1998.

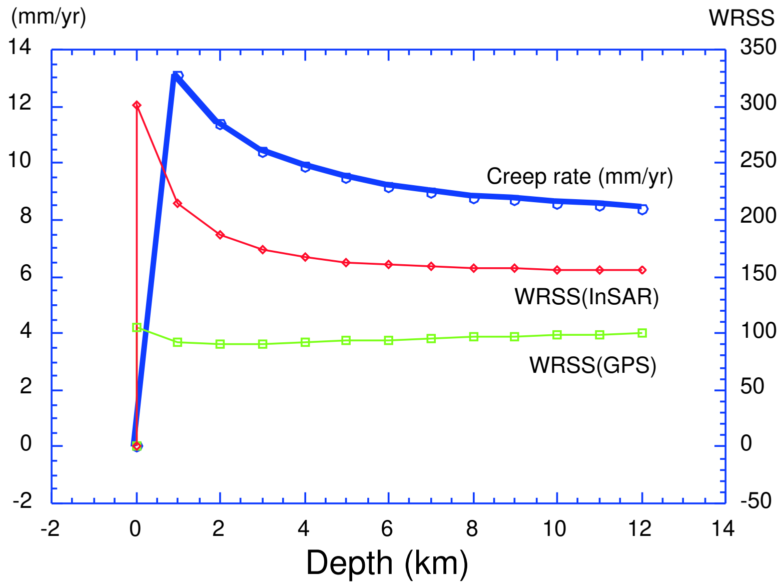

Figure 10.18: Misfit (WRSS) and creep rates from joint inversion of GPS and InSAR data as a function of depth of uniformly creeping model fault. Misfits (thin lines) are shown separately for InSAR and GPS data. Note that while the InSAR data favor creep to greater depths, the GPS data do not have a pronounced minimum. The best-fitting creep rates of 8-10 mm/yr for depths > 5 km (bold line) are higher than those observed at the surface.

9. Modeling surface creep on the Hayward fault using rate-and-state friction

David Schmidt and Roland Bürgmann

Induced creep was documented on several Bay Area faults following the 1989 Loma Prieta earthquake. Various responses were observed ranging from accelerated/decelerated creep to a temporary reversal in slip direction (*Galehouse*, 1997). Larger events, such as the 1906 San Francisco earthquake, are expected to include significant postseismic transients thereby imposing a time-dependent creep response on adjacent faults. We explore the possibility of induced creep on the Hayward fault following the 1906 event using a rate-and-state constitutive law to model the temporal slip response given a time-dependent loading curve.

This analysis requires advance knowledge of various fault parameters used to specify the rate-and-state formulation (*Linker et al.*, 1992). We invert for the A and B parameters which define the weighting of velocity and state dependence, respectively, using the creep response observed along the Hayward fault following Loma Prieta. In addition, a temporal loading curve is calculated using a finite element code to model the coseismic stress change and the postseismic relaxation (*Kenner et al.*, 1998). Various models representing different structural geometries of the Bay Area are tested. With these inputs we then calculate the temporal creep response along the southern Hayward fault for each model. The rate-and-state formulation predicts induced left lateral creep along the Hayward fault for all structural models. No detailed observations of creep were made immediately following the 1906 rupture that can confirm nor refute our model predictions. Offset cultural features which record the net displacement are used to constrain the average slip rate observed over a range of time periods since 1906 (*Lienkaemper et al.*, 1997). These data suggest that averaged creep rates along the Hayward fault have remained nearly constant since about 1920 until Loma Prieta in 1989. Given the available data, we find that the left-lateral creep predicted by our modeling is acceptable under the condition that right lateral creep resumes by the 1920's.

Each model produces varying creep signatures which allow us to discriminate between the different shear-zone geometries. Three different rheological models are used to compute the stressing history imposed on the Hayward fault following the 1906 event (Figure 10.19). Both a purely elastic model and an elastic model that includes vertical shear zones beneath the San Andreas, Hayward, and Calaveras faults produce a transient left-lateral response followed by a return to the secular right lateral creep rate in 20 to 40 years. A model that includes a horizontal shear zone at a depth of 15 km predicts a prolonged initial left-lateral response with a slow return to the secular slip rate over a century. Our modeling suggests that in future seismic events, surface creep records could provide an additional source of information to discriminate between differing models of upper crustal rheology.

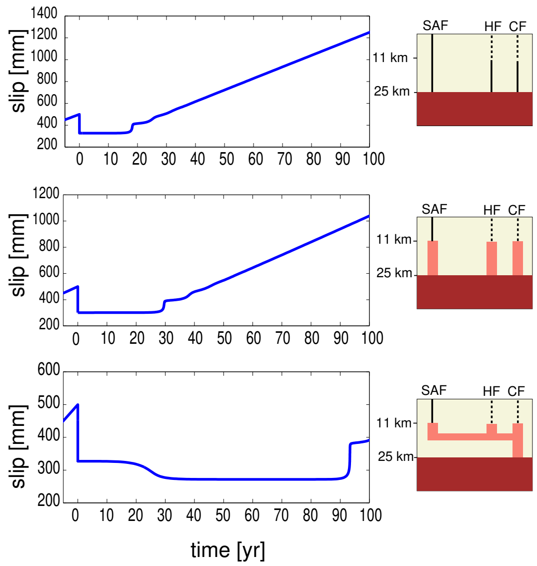

Figure 10.19: The above plots show modeled surface creep for various rheological models shown on the right. The top result is for an elastic model while the middle plot uses a vertical shear zone model. The bottom plot uses a shear zone model that includes a horizontal shear zone connecting the three major faults.

9.1 Acknowledgments

Special thanks to Jon Galehouse for providing surface creep measurements along the Hayward fault.

9.2 References

Galehouse, J. S., Effect of the Loma Prieta earthquake on fault creep rates in the San Francisco Bay region, *U. S. Geological Survey Professional Paper* 1550D, 193-207, 1997

Kenner, S., and P. Segall, Time-dependence of the stress shadowing effect and its relation to the structure of the lower crust, *Geology*, 27, 2, p. 119-122, 1999

Lienkaemper, J. J., and J. S. Galehouse, Revised long-term creep rates on the Hayward fault, Alameda and Contra Costa counties, California, *USGS open-file report* 97-690, 1997

Linker, M.I., and J. H. Dieterich, Effects of variable normal stress on rock friction: observations and constitutive equations, *J. Geophys. Res.*, 97, pp. 4923-4940, 1992

10. Research Projects under Lane Johnson

10.1 Effect of damage on explosion generated elastic waves

L. R. Johnson and C. G. Sammis

A basic study was completed on the effect that rock damage has on the elastic waves generated by explosions. This work was done in collaboration with Charles Sammis at the University of Southern California. The basic idea of this research was to study the effects of pre-existing cracks in the region of high stresses immediately surrounding explosive sources. Such cracks are present in almost all rocks and occur at a variety of scales. Sammis, working with Ashby at Cambridge University, has developed a quantitative micro-mechanical model of how such cracks could grow as a function of the local stress field. The first step was to calculate the stress field surrounding an explosive source and this was accomplished with an equivalent elastic method. Comparisons with data from the 1 kt chemical explosion of Non-Proliferation Experiment showed that the stress levels and the waveforms generated with this method were reasonable simulations of realistic observations in the field. Then it was shown that these stresses were capable of causing a growth of pre-existing cracks in a fairly large volume surrounding the explosion, with a radius up to ten times that of the original explosion cavity. The effects of the density of pre-existing cracks and their size was studied, with the main conclusion being that the volume of crack growth increases with the initial size of the cracks. The second main result of this research was to develop a method for calculating the secondary elastic waves generated by the growth of pre-existing cracks, which involved developing the appropriate moment tensor representation of the cracks and then summing the contributions of all the cracks using Green functions. It was found that, while the contribution from an individual crack is small, the combined effect of many cracks in a large volume can generate secondary waves that are comparable in amplitude to the primary waves generated by the explosion. Most importantly, provided there is some asymmetry in the pattern of crack growth, this process is quite effective in generating S waves, thus providing a quantitative explanation of how S waves can be generated by an explosion. Two types of asymmetry, a shear pre-stress and a preferred orientation, were investigated and both proved to be effective in generating S waves in the far field.

10.2 Dynamic composite media theory

B. Kaelin and L. R. Johnson

Considerable progress has been made on the basic problem of characterizing the elastic and anelastic properties of a material from a knowledge of the relative proportions of its components. In the past this approach has been successful in estimating elastic properties in the quasi-static limit, where it goes by the names of effective media theory or composite media theory. However, such approaches are not sufficient for the high frequencies that are commonly encountered, so we have been developing a more complete theory which is applicable over a broad frequency range. So far the results are quite promising with respect to the handling of the elastic moduli, density, porosity, and pore fluids. Two papers describing the general approach have been published. The first paper describes a dynamic composite elastic medium theory for one-dimensional media. The method is self-consistent, is valid for all frequencies, and agrees with known solutions at both low and high frequencies. The comparison with complete numerical solutions for the one-dimensional problem allows a rigorous evaluation of the method. The second paper extends the dynamic composity elastic medium theory to three-dimensional media. In this case the method is also self-consistent, is valid for all frequencies, and agrees with known solutions at low frequency. The method requires the calculations of complete scattering solutions, and such calculations have been done for the case of spherical inclusions.

10.3 Source parameters of small earthquakes

C. G. Sammis, R. M. Nadeau, and L. R. Johnson

Our earlier studies of the source parameters of small earthquakes estimated from moment release rates has been extended in a collaborative study with Professor Charles Sammis at the University of Southern California. Laboratory results concerning the strength of rocks and asperity models of friction were studied and compared with the earthquake data. The study shows that these two different types of data are consistent and imply a discrete hierarchical fractal distribution of asperities having a fractal dimension of 1.0 and a discrete rescaling factor of 10.

10.4 Three-dimensional velocity structure of the earth

D. W. Vasco, O. Marques, and L. R. Johnson

Our recent studies of the three-dimensional structure of the earth have relied upon the tomographic inversion of large amounts of high frequency seismic travel time data. Although various approaches to this type of problem have been used, with the major differences involving the parameterization of the model and regularization, all of the methods require the solution of a very large inverse problem. Unfortunately, these problems are so large that the available computer resources are generally sufficient to provide an estimate of the solution only, and it is rare that these solutions can be provided with formal estimates of resolution and uncertainty. Various approximate estimates of resolution and uncertainty have been proposed and used, but it can be demonstrated that these are not entirely adequate. We have been able to overcome this deficiency by developing a procedure where the eigenvalues and eigenvectors associated with a singular value decomposition of the problem can now be calculated for problems with the order of 10^5 model parameters. The procedure makes use of an iterative Lanczos algorithm, and has been implemented for both work stations and large parallel computers.

10.5 Use of Genetic Algorithms in Geophysical Inverse Problems

P. B. Parker and L. R. Johnson

Genetic algorithms offer an attractive approach for many geophysical inverse problems in that they can explore the entire model space, are not dependent upon an initial estimate, require no derivatives, and are much more efficient than completely random search methods. What has been lacking has been an understanding of how this approach performs on realistic geophysical inverse problems and how the control parameters influence the performance. It has been found that a particular choice of parameters consistently produces optimal results for a broad range of problem difficulties. At least for problems of the type encountered in geophysics, the choice of a low mutation rate of about half the inverse of the population size was the most critical factor, with the crossover method and rate having a relatively minor affect upon performance. Tournament selection was found to be the most effective and robust selection method. In addition to an investigation of the general performance of genetic algorithms, the method has been applied to practical problems of modeling receiver functions and interpreting gravity data.

10.6 Calculation of waveforms in three-dimensional media

H. Keers and L. R. Johnson

For the purpose of modeling elastic wave propagation in media which are heterogeneous in three dimensions, there is a need for approaches which are intermediate between expensive numerical methods such as finite differences and overly-simplified methods such as geometrical ray theory. The WKBJ approach is such a method, but it is suitable only for media inhomogeneous in one dimension. We have been investigating semi-analytical methods of the Maslov type in an attempt to develop an approach which includes most of the relevant wave phenomena and also makes reasonable demands upon computing resources. Progress has been made by using Kirchoff-Helmholtz theory to develop a method which includes non-stationary ray paths and properly accounts for caustics. Sensitivity functions have also been generated, which allows the method to be used in waveform inversion problems. Both forward and inverse applications of this method have been studied and it has been tested with a tomographic inversion of data collected in the laboratory. Including the waveforms leads to a significant improvement over inversions that use only travel times.

10.7 References

Dicke, M., *Seismicity and Crustal Structure at the Mendocino Triple Junction, Northern California*, M.S. Thesis, University of California, Berkeley, 79 pp., 1998.

Glaser, S. D., G. G. Weiss, and L. R. Johnson, Body waves recorded inside an elastic half-space by an embedded, wideband velocity sensor, *J. Acoust. Soc. Am.*, **104**, 1404-1412, 1998.

Kaelin, B., and L. R. Johnson, Dynamic composite elastic medium theory. Part I., One-dimensional media, *J. Appl. Phys.*, **84**, 5451-5457, 1998.

Kaelin, B., and L. R. Johnson, Dynamic composite elastic medium theory. Part II., Three-dimensional media, *J. Appl. Phys.*, **84**, 5458-5468, 1998.

Kaelin, B., and L. R. Johnson, Using seismic crosswell surveys to determine the aperture of partially water-saturated fractures, *Geophysics*, **64**, 13-23, 1999.

Parker, P. B., *Genetic Algorithms and Their Use in Geophysical Problems*, Ph.D. Thesis, University of California, Berkeley, 202 pp., 1999.

Sammis, C. G., R. M. Nadeau, and L. R. Johnson, How strong is an asperity?, *J. Geophys. Res.*, **104**, 10,609-10,619, 1999.

Vasco, D. W., L. R. Johnson, and O. Marques, Global earth structure: inference and assessment, *Geophys. J. Int.*, **137**, 381-407, 1999.

Chapter 11

Ongoing Research - Global

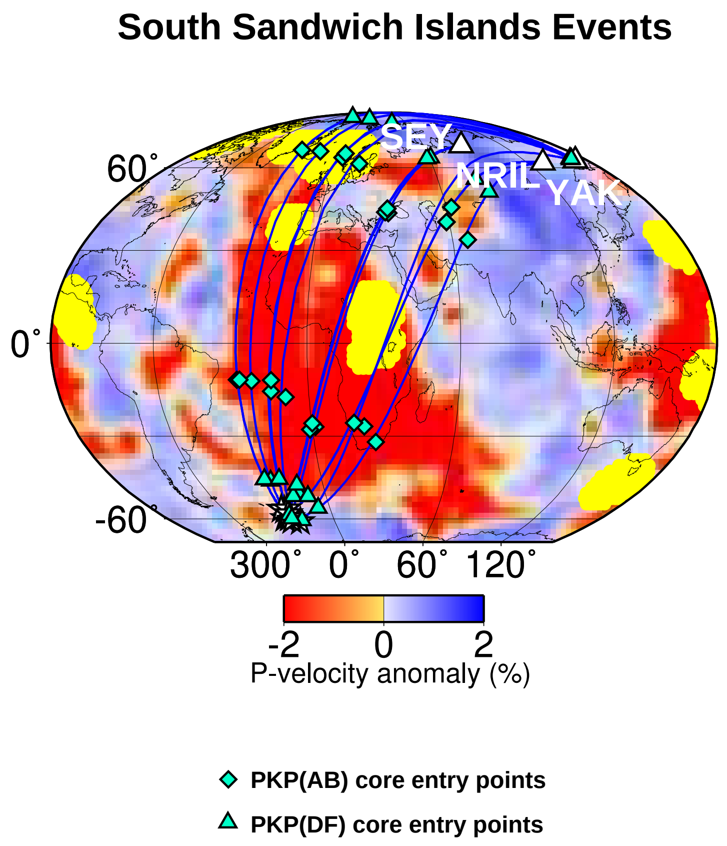

1. The effect of D" on PKP(AB-DF) travel time residuals and possible implications for inner core structure

Hrvoje Tkalčić, Ludovic Bréger, and Barbara Romanowicz

The hypothesis that the bulk of the inner core is anisotropic is based on PKP travel time observations (Morelli, A. and A. M. Dziewonski, 1986) and splitting in free oscillation data (Woodhouse et al., 1986). Anisotropy in the inner core with the fast axis in the direction of earth's spin axis should cause a faster propagation of PKP(DF) waves that travel parallel to spin axis than those which traverse the inner core in an equatorial plane (e.g. Creager, 1992). However, the number of very anomalous paths quasi-parallel to the Earth's rotation axis is relatively small due to uneven global distribution of large earthquakes and seismographs. We analyse a global dataset of PKP(AB-DF) travel times residuals, and discuss their significant dispersion ($\pm$ 2s), and coherent large scale patterns. As found from global tomographic studies, the lowermost mantle contains two major very slow, large scale anomalous domains: one beneath the Central Pacific, and one beneath Africa. PKP(DF) waves dive at steep angles into the core, while PKP(AB) graze the CMB at large distances, diffract over a few degrees, and can accumulate large residuals in the strongly heterogeneous D". In an attempt to forward model our observations, we assumed (as in Bréger, L. and B. Romanowicz, 1998) that slow velocities were strongly underpredicted under the Pacific and Africa, and increased their amplitude in the bottom 400 km of the mantle, while not changing their shape (we used the tomographic model from S. Grand et al., 1997 as the reference model). Furthermore, in the computation of synthetic AB and DF residuals, we included the effect of Ultra Low Velocity Zones (ULVZs) in places where they have been reliably documented (hereafter, this modified model is called MMM). One possible scenario is a propagation of PKP(DF) phase through a normal to fast heterogeneous region in the lowermost mantle, while PKP(AB) experiences some large delays due to a consistently very slow anomaly. This, we believe, is the case for quasi-polar paths from South Sandwich Islands events to northern Eurasia. This type of path happens to correspond to a geometry for which PKP(AB) spends most of its time in the lower mantle within the large African slow anomaly (Fig. 1), while PKP(DF) misses the zone of strongly reduced velocity. We showed that the trends observed for quasi-equatorial paths are consistent with predictions from recent tomographic mantle models, when the latter are modified to account for strong heterogeneity at the base of the mantle under the Pacific Ocean and Africa, as described above (Fig. 2).

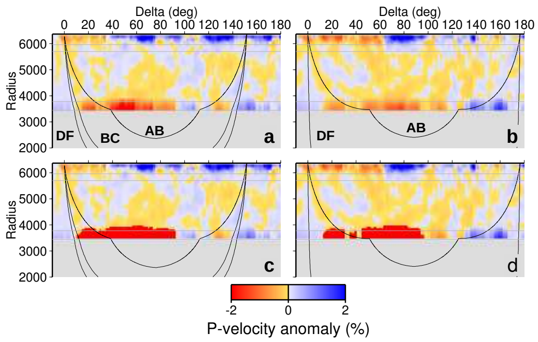

Figure 11.1: a) Cross section through the original tomographic model for a path between South-Sandwich Island event 93/01/10 (-59.42^oN -25.78^{o}E 33km) and station NRIL (distance 151.50^o). Also plotted are AB, BC, and DF raypaths. (b) Same as (a) for a path to station SEY (distance 176.37^o). Also plottedare the AB and DF raypaths (BC does not exist at this distance). (c) and (d) Same as (a) and (b) for the modified MMM velocity model.

Likewise, for polar paths, we show that a large part of the signal could be explained by deep mantle structure (Fig. 2). Although such a simple model does not explain all data, our goal to demonstrate a possible strong contamination of PKP(AB-DF) residuals by the deep mantle structure, has been achieved.

There has been a lack of consensus as to the details of anisotropic structure in the inner core. We believe that the contamination of inner core sensitive data by structure at the bottom of the mantle may have been generally underestimated, and that future efforts to derive realistic models of inner core structure will have to accurately account for such effects. The effects of complex structure in the deep mantle on PKP(AB-DF) travel times should be carefully considered in order to reliably estimate the anisotropic or/and heterogeneous structure of the inner core.

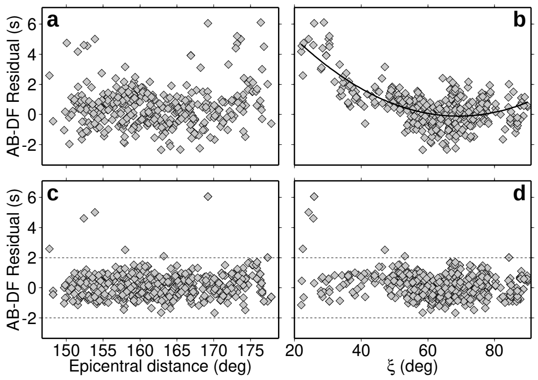

Figure 11.2: AB-DF differential travel time residuals as a function of epicentral distance (a) and angle ξ of the path in the inner core with respect to the rotation axis (b). The best fitting second degree polynomial in $cos^2\xi$ (solid line) was added in (b) to outline the observed trend. Such a trend is expected, at fixed distance, for models of constant cylindrical anisotropy in the inner core with axis parallel to the rotation axis. (c) and (d): Same as (a) and (b) after correction for the MMM model discussed in the text. Mean residuals are 1.05 and 0.67, with rms 0.10 and 0.06 respectively, before and after correction using MMM. Note that a few large residuals at low ξ remain unexplained. These correspond to South Sandwich Islands paths to stations COL and BILL. The complexity of these particular paths has been noted previously, for instance, BC-DF residuals differing by more than 2s for neighbouring stations.

1.1 Acknowledgments

We thank Michael Wysession for helpful discussions, and the IRIS, CNSN, Geoscope, GRSN, Mednet, BDSN, and SCSN teams.

1.2 References

Bréger, L. and B. Romanowicz, Three-Dimensional structure at the base of the mantle beneath the Central Pacific, *Science 382*, 718-720, 1998.

Bréger, L., H. Tkalčić and B. Romanowicz, The effect of D" on PKP(AB-DF) travel time residuals and possible implications for inner core structure, submitted to *EPSL*.

Creager, K. C. Anisotropy of the inner core from differential travel times of the phases PKP and PKIKP, *Nature 356*, 309-314, 1992.

Grand, S., R. van der Hilst, and S. Widiyantoro, Global seismic tomography; a snapshot of convection in the Earth, *G.S.A. Today 7*, 1-7, 1997.

Morelli, A. and A.M. Dziewonski, Anisotropy of the core inferred from PKIKP travel times, *Geophys. Res. Lett. 13*, 1545-1548, 1986.

Woodhouse, J.H., D. Giardini, and X.-D. Li, Evidence for inner core anisotropy from splitting in free oscillation data, J. H., D. Giardini, and X.-D. Li, *Geophys. Res. Lett. 13*, 1549-1552, 1986.

2. New constraints on deep earth heterogeneity and anisotropy from PKP(BC-DF) travel times

Ludovic Bréger, Hrvoje Tkalčić, and Barbara Romanowicz

2.1 Introduction

Proposed thirteen years ago [*Morelli et al.*, 1986; *Woodhouse et al.*, 1986], the anisotropy of the earth's inner core seems today firmly established, the fast axis of iron crystals being roughly aligned with the earth's axis of rotation. Yet, there is still no consensus as to what the exact distribution and strength of this anisotropy are. Most studies of the structure of the inner core are based on PKP travel times, and in particular differential travel times such as PKP(AB-DF) and PKP(BC-DF), which are often used in order to reduce mantle effects. We have showed that AB-DF differential travel times could actually be largely explained by deep mantle structure, including the trend with angle of the path with respect to the earth's rotation axis, usually attributed to inner core anisotropy [*Bréger et al.*, 1999]. Although BC-DF travel times are in principle much less sensitive to mantle structure, it is nevertheless important to quantify the effect due to heterogeneity in the earth's mantle to reliably estimate the signal due to the inner core.

2.2 Short-scale variations of BC-DF travel times

By fixing a station and comparing residuals in a given source region, it is possible to gain insight into small scale spatial variations of BC-DF residuals. Station COL, in Alaska, is unfortunately the only one for which a relatively large dataset of hand-picked BC-DF travel times on quasi-polar paths is available. International Seismological Center (ISC) bulletins provide a large dataset spanning several decades. One drawback of this dataset is that it is very noisy. However, it has recently been improved by systematic elimination of misidentified phases and earthquake relocation [*Engdahl et al.,* 1998]. From this improved catalog, we have extracted BC and DF absolute travel time residuals with respect to the ak135 model [*Kennett et al.*, 1995] for a number of key stations corresponding to polar paths and classified them by source region (Figure 11.3). A second drawback of the ISC dataset is that measurements of both BC and DF travel times for the same event/station pair are infrequent. However, when absolute DF and BC residuals show systematic trends as a function of epicentral distance and angle ξ, it is possible to estimate the corresponding variations of BC-DF and their standard deviations in a "composite" fashion.

In Figure 11.4 are summarized the trends which we observed for 10 quasi-polar paths. We have plotted the composite BC-DF travel time anomalies as a function of angle ξ (Figure 11.4), compared to predictions from different simple models of inner core anisotropy. Figure 11.4 shows large excursions, both locally and over the range of ξ considered, from a trend that is compatible with the predictions of a model of anisotropy with strength on the order of 1.5%, at least for the top 400km of the inner core.

In order to explain our observations, a very complex model of inner core anisotropy, possibly associated with heterogeneity, needs to be invoked. The inner core structure would change on a hemispherical scale [*Tanaka and Hamaguchi*, 1997], but also over distances of a few hundreds of kilometers, from one station to another, and on even shorter scales, when the station is fixed. Some very large residuals are sometimes observed: hand-picked residuals at station COL vary from 2s to exceptional values of some 5s. An anisotropy of more than 5% would be required in order to speed up DF by 5s at 154^o. This is extremely high, but could be compatible with the results of recent high-pressure experiments [*Mao et al.,* 1998] ,and the existence of a complex convective pattern [*Jeanloz and Wenk*, 1988].

A complex lowermost mantle structure could be an alternative explanation to this complex behaviour. BC-DF travel times are not anomalous for polar paths for roughly one third of the globe, over Asia and Russia [*Tanaka and Hamaguchi*, 1997]. Interestingly, the deep mantle beneath these regions seems weakly anomalous. On the other hand, some of the largest residuals are obtained at station NRIL, for which there could be a strong interaction of the PKP paths with the base of the African plume (Figure 11.3).

The rapid variations of BC-DF residuals on scales of a few hundreds kilometers can be understood as an effect of very complex anisotropic structure at the top of the inner core, or mantle heterogeneity, or a combination of both. Lowermost mantle structure happens to geographically correlate with the complex behaviour of BC-DF residuals, in locations where it is well documented. Whatever their origin, the existence of such strong variations shed a new light on the complexity of the deep earth.

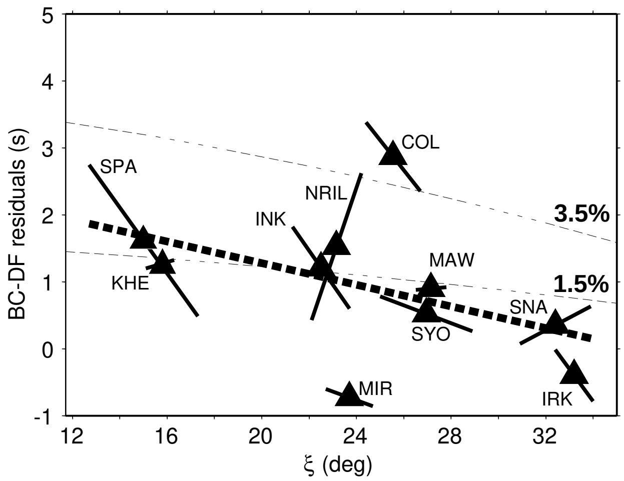

Figure 11.4: Summary of the estimated variations of BC-DF travel time residuals for polar paths. Triangles represent the mean values of the extrapolated residuals, and the thick black lines their variations as a function of ξ. The thick dashed line represents the average observed linear trend, and is compared with the predictions for 3.5% and 1.5% anisotropy (thin dashed lines) at 148^o epicentral distance.

2.3 Acknowledgments

We are particularly grateful to A. Souriau and G. Poupinet, M. Wysession, P. Richards, and S. Tanaka and H. Hamaguchi for providing us with their data, and E. R. Engdahl, R. van der Hilst, and R. Buland for making their ISC dataset available. We benefited from discussions with H.R. Wenk and R. Jeanloz. We also thank the IRIS, CNSN, Geoscope, GRSN, Mednet, BDSN, SCSN, and GRSN teams.

2.4 References

Bréger, L., H. Tkalcic, and B. Romanowicz, The effect of D" on PKP(AB-DF) travel time residuals and possible implications for inner core structure, Submitted to *Earth Planet. Sci. Lett.*, 1999.

Engdahl, E.R., R. van der Hilst, and R. Buland, Global teleseismic earthquake relocation with improved travel times and procedures for depth determination, *Bull. Seismol. Soc. Am.*, *88*, 722-743, 1998.

Garnero, E.J., J. Revenaugh, Q. Williams, T. Lay, and L.H. Kellogg, *The Core-Mantle boundary*, Ed. Gurnis, M., Buffett, B.A., Knittle, E. and M. E. Wysession, 319-334, American Geophysical Union, Washington, DC, 1998.

Grand, S., R. van der Hilst, and S. Widiyantoro, Global seismic tomography: a snapshot of convection in the Earth, *G.S.A. Today*, *7*, 1-7, 1997.

Kennett, B.L.N., E.R. Engdahl, and R. Buland, Constraints on seismic velocities in the Earth from travel times, *Geophys. J. Int.*, *122*, 108-124, 1995.

Jeanloz, R. and H.R. Wenk, Convection and anisotropy of the inner core, *Geophys. Res. Lett.*, *15*, 72-75, 1988.

Mao H., J. Shu, G. Shen, R.J. Hemley, B. Li, and A.K. Singh, Elasticity and rheology of iron above 220 GPa and the nature of the Earth's inner core, *Nature*, *396*, 741-743, 1998.

Morelli, A., A.M. Dziewonski, and J.H. Woodhouse, Anisotropy of the core inferred from PKIKP travel times, *Geophys. Res. Lett.*, *13*, 1545-1548, 1986.

Tanaka, S., and H. Hamaguchi, Degree one heterogeneity and hemispherical variation of anisotropy in the inner core from PKP(BC)-PKP(DF) times, *J. Geophys. Res.*, *102*, 2925-2938, 1997.

Woodhouse, J.H., D. Giardini, and X.-D. Li, Evidence for inner core anisotropy from splitting in free oscillation data, *Geophys. Res. Lett.*, *13*, 1549-1552, 1986.

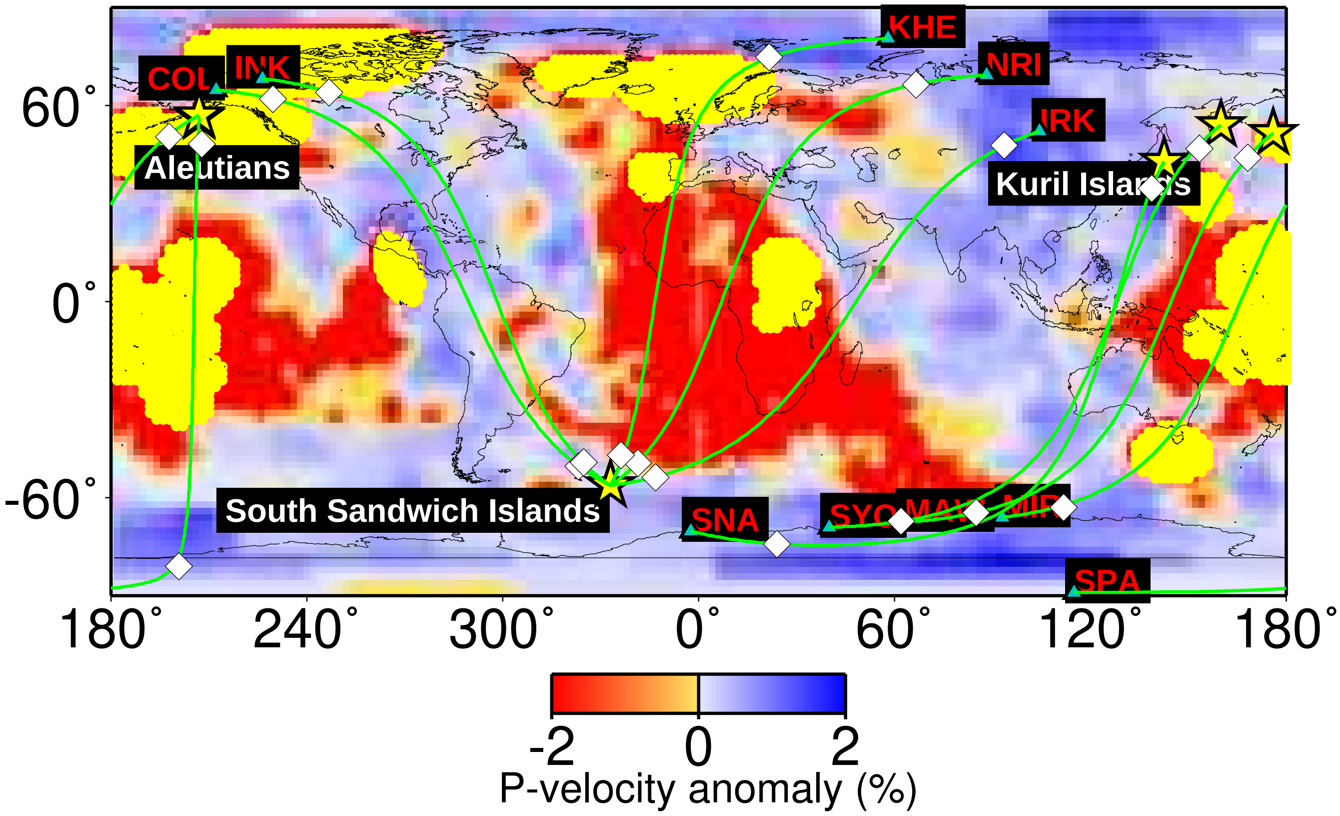

Figure 11.3: Near polar source-receiver paths analysed in this study. Stations, source regions, and great circle paths are indicated by blue triangles, yellow stars, and green lines respectively. Plotted as background is Grand et al.'s [1997] tomographic model for which we have converted S-velocity to P-velocity using the scaling dlnVs/dlnVp=2. This model was found to be a good starting point to describe the large scale distribution of P-velocity in D" on the global scale [*Bréger et al.,* 1999], including low velocity regions in the Pacific and under Africa. Yellow patches indicate the regions where Ultra Low Velocity Zones [*Garnero et al.,* 1998] have been detected. Outer core DF penetration points are indicated by white diamonds.

3. Anomalous splitting of core sensitive modes: a reevaluation of possible interpretations

B. Romanowicz and L. Bréger

3.1 Introduction

Inner core anisotropy was proposed 13 years ago to explain two categories of intriguing observations: (1) faster propagation times for seismic body waves that travel through the inner core along paths quasi-parallel to the earth's rotation axis, than for those that travel on equatorial paths (Poupinet et al., 1983; Morelli et al., 1986), and (2) anomalous splitting of core-sensitive free oscillations (Masters and Gilbert, 1981; Woodhouse et al., 1986). These observations have been confirmed in many subsequent studies (e.g. Shearer, 1991; Creager, 1992; Vinnik et al., 1994; Su and Dziewonski, 1995) and models of inner core anisotropy have been progressively refined. These models were originally cast in terms of constant transverse isotropy with fast axis parallel to the earth's rotation axis, for which an interpretation in terms of alignment of hcp-Fe crystals was proposed. Over the years, inner core anisotropy models have become more complex. Depth dependence was introduced (Su and Dziewonski, 1995; Tromp, 1993) and more complex spatial dependence suggested (Li et al., 1991; Romanowicz et al., 1996; Durek and Romanowicz, 1999). Most recently, several studies have proposed even stronger departures from simple models of inner core anisotropy. An asymmetry in the anisotropy pattern was pointed out (Tanaka and Hamaguchi, 1997; Creager, 1999), with one "quasi-hemisphere" of the inner core anisotropic and the other not, and it has been argued that the top 100-200 km of the inner core may be isotropic and laterally varying (Song and Helmberger, 1998). Strong, small scale variation in the anisotropy along a highly anomalous path between the South Sandwich Islands and station COL in Alaska has also been documented (Creager, 1997).

The necessity to modify the simple original model of constant anisotropy, and introduce significant complexity, has become quite clear. Moreover, we have recently proposed that an important contribution to the trend of travel time residuals, as a function of angle of the path with respect to the rotation axis, for PKP(AB)-PKP(DF) data, could come from strong heterogeneity in D" (Bréger et al., 1999a) and we proposed a possible trade-off between D" structure and inner core anisotropy in the interpretation of differential PKP travel time data (also PKP(BC)-PKP(DF), Bréger et al., 1999b).

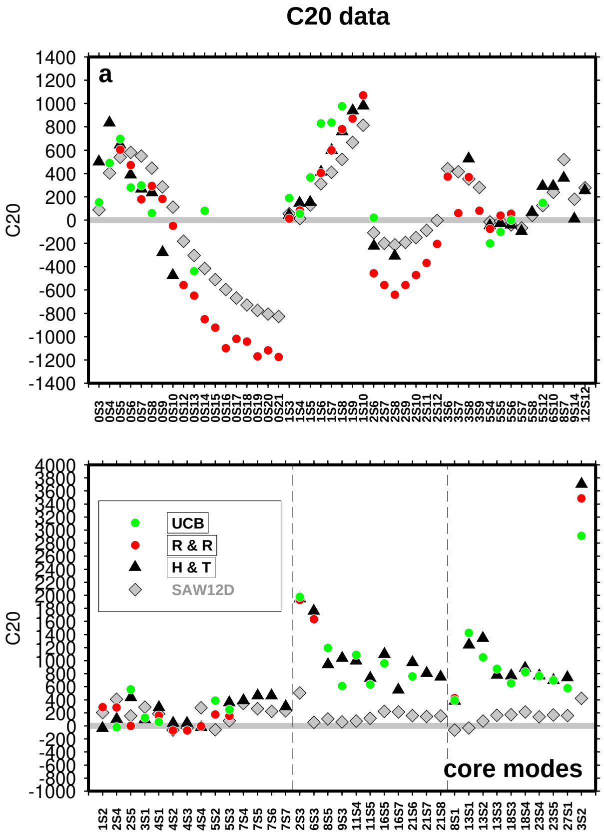

Figure 11.5: Splitting data for C20, relative to the center frequency, in 10^{-6} units (cf He and Tromp, 1996) from various sources, and predictions for a global tomographic model of the mantle (SAW12D). UCB: from Durek and Romanowicz (1999); *R&R*: from Resovsky and Ritzwoller (1998); *H&T*: from He and Tromp (1996). (a) "mantle modes"; (b) "core modes". The core modes have been subdivided (vertical broken lines) into those that have no sensitivity to inner core structure (1S2-7S7), those that have small sensitivity to inner core structure (2S3-21S8) and those that have more than 4% of their energy in the inner core (8S1-3S2).

Even if we accept an interpretation of PKP observations in terms of a complex inner core anisotropy model, some of the recent observations are in contradiction with the normal mode splitting observations. Indeed, since normal modes are primarily sensitive to even order structure, it is difficult to reconcile the hemispherical model (Tanaka and Hamaguchi, 1997; Creager, 1999) with the dominant zonal "C20" component of anomalous splitting observations. Likewise, since modes are primarily sensitive to the uppermost third of the inner core, their splitting becomes more difficult to explain in terms of anisotropy if there is an isotropic layer several hundred km thick at the top of the inner core (Durek and Romanowicz, 1999).

Alternative interpretations for anomalous mode splitting have been proposed in terms of outer core heterogeneity (Ritzwoller et al., 1988; Widmer et al., 1992).

In view of the recent controversies regarding the level and complexity of inner core anisotropy, we have decided to reexamine the issue of interpretation of anomalous mode splitting data. We are assisted in this process by the recent accumulation of high quality low frequency data, owing to the expansion of the global digital broadband network and the occurrence of several very large deep earthquakes, in particular the M8.2 Bolivia earthquake of June 9, 1994.

3.2 Data Analysis

We have assembled a spheroidal mode splitting dataset for 79 normal modes sensitive either primarily to structure in the mantle (42 modes) or both to structure in the mantle and in the core (37 modes). These data are tabulated in terms of measured splitting coefficients, as defined below, from three sources: measurements by Resovsky and Ritzwoller (1998) mostly for mantle modes, by He and Tromp (1996) for a combination of mantle and core modes, complemented by our own dataset, primarily for core modes (Durek and Romanowicz, 1999).

Figure 11.5 shows a comparison of C20 measurements from the 3 sources considered, giving a sense of uncertainty on the splitting measurements. In most cases, agreement between different groups are excellent (also with measurements from Laske and Masters, personal communication). We have distinguished mantle modes (top panel) and modes with significant sensitivity to core structure (bottom panel). We classify the latter into "outer core" modes ("oc"), that are not sensitive to inner core structure, and two categories of "inner core" modes: (1) those with less than 4% sensitivity to inner core structure (modes 2S3-21S8, category "ic1") and (2) those with stronger sensitivity to inner core structure (modes 8S1-3S2, category "ic2"). Mode 3S2 has been assigned to category "ic2", only because it has significant sensitivity to S-velocity in the inner core. We will single out this particular mode, which exhibits the strongest anomalous splitting, the largest uncertainties in the measurements, as well as the largest sensitivity to inner core anisotropy. We have also plotted the splitting predictions of mantle model SAW12D (Li and Romanowicz, 1996), an SH-model of the mantle, obtained using body and surface waveform data. In converting the S-velocity from this model to density (ρ) and P-velocity (Vp), we have assumed standard conversion factors: $dlnVp/dlnVs = 0.5$ and $dln\rho/dlnVs = 0.25$, as proposed by Li et al. (1991). Predictions for other mantle models are similar. Two observations are striking: for mantle modes, the predictions of SAW12D follow the data quite closely for all branches, although the amplitudes in the 0S and 1S branches are underpredicted. For core sensitive modes, we note, as previous authors, that the mantle model predicts practically no splitting for modes with any sensitivity to inner core structure, whereas the data consistently show a high level of splitting. This is referred to in the literature as "anomalous" splitting. We note that, except for mode 3S2, the level of splitting observed for modes in categories ic1 and ic2 is comparable, with a few modes exhibiting somewhat larger splitting in both datasets (2S3 and 6S3 in ic1 and 13S1, 13S2 in ic2).

3.3 Inversion results

We invert these data using the following parametrization. We consider simple layered models of Vs, Vp and ρ in the mantle (Table 1), Vp and ρ in the outer core, as well as models of inner core anisotropy with various levels of complexity, as allowed by the axisymmetric formalism developed by Li et al. (1991) and applied more recently to broadband data (Romanowicz et al., 1996; Durek and Romanowicz, 1999). We also include topography on three discontinuities (Moho, 670 km discontinuity and core mantle boundary (CMB)). In order to better assess where the inversions naturally tend to put the structure, we do not apply smoothness constraints, only overall damping, as needed, and have, after some experimentation, arrived at a layer parametrization which yields stable inversions of mantle modes without smoothing (5 layers in the crust/upper mantle, 12 layers in the lower mantle). In the upper mantle, we invert for Vs only, assuming Vp and ρ to be proportional to Vs, consistent with findings of independent studies based on normal modes and travel times (Robertson and Woodhouse, 1995; Su and Dziewonski, 1997; Ishii and Tromp, 1998; Kuo et al., 1998). In the lower mantle, we solve separately for Vs,Vp and ρ. Previous studies have shown that the proportionality between Vp and Vs breaks down below a depth of 1800-2000km, which may result in different depth profiles for C20 in Vs, Vp and ρ respectively (Robertson and Woodhouse, 1995; 1996; Bolton and Masters, 1996; Ishii and Tromp, 1998; Kuo et al., 1998).

In the outer core, we consider one or several layers, and solve for Vp and ρ without any a-priori constraints on the ρ structure, or the absence thereof. Several one layer models are considered, with increasing thickness, starting from the top (or the bottom) of the outer core.

Three parametrizations of inner core anisotropy are considered: (1) a simple constant transverse anisotropy model (3 independent variables, "i1 models"), (2) a model of transverse anisotropy with depth dependence, described by a polynomial in r^2 up to degree 4 (15 independent variables, "i2 models") and (3) a more general axisymmetric model including lateral variations expressed in spherical harmonics up to degree 4 (44 independent parameters, "i3 models"). We note that for the latter model, the inverse problem, with a total of 88 parameters, is under- determined. We consider results of inversions for 12 different depth parametrizations: 1-mantle only, 2-9 - mantle and outer core, 10-12 - mantle and inner core anisotropy.

Figure 11.6 shows the residual variance in the C20 coefficient data as a function of model number, when different subsets of modes are considered. When mode 3S2 is excluded from the dataset, our results indicate that outer core models provide much better fit to the data than models with inner core anisotropy. When mode 3S2 is included, the overall fit according to residual variance is better for inner core anisotropy models, however, this reflects primarily a better fit to the very anomalous splitting of 3S2, whereas the fit to other core and mantle modes is not significantly improved.

The results of our study can be summarized as follows: (1) inner core anisotropy improves the overall fit to data compared to a model with aspherical structure restricted to the mantle; (2) when mode 3S2 is excluded from the dataset, simple models with heterogeneity in the outer core fit the data consistently better than simple inner core anisotropy models; (3) when mode 3S2 is included, overall residual variances are smallest or inner core anisotropy models. However, the splitting of 3S2 is fit at the expense of that of the 5S mantle mode branch, sensitive to P-velocity in the mantle. (4) outer core models are more stable and consistent with each other than inner core models, when different subsets of core modes are inverted (i.e. modes with small versus large sensitivity in the inner core).(5) Lateral heterogeneity in the mantle alone (in particular D") cannot consistently account for the splitting of all modes.

Simple anisotropic models of the inner core are therefore not sufficient to simultaneously explain the splitting of spheroidal mantle and core modes, and a combination of deep mantle and outer core structure contributes significantly to the pattern of splitting. The outer core structure retrieved is consistent with either heterogeneity associated with the Taylor cylinder tangent to the earth's inner core, or the possible existence of a stagnant layer at the top of the outer core, enriched in light material. In the latter case, we conjecture that a small amount of shear could help reconcile the large splitting of 3S2 with that of other core and mantle modes. Such models deserve further investigation.

3.4 References

Bréger, L., H. Tkalcic, and B. Romanowicz, The effect of D" on PKP (AB-DF) travel time residuals and possible implications for inner core structure, in revision *E.P.S.L.*, 1999.

Bréger, L., B. Romanowicz, and H. Tkalcic, PKP(BC-DF) travel times residuals and short scale heterogeneity in the deep earth, *Geophys. Res. Lett.*, in press, 1999.

Creager, K.C., Anisotropy of the inner core from differential travel times of the phases PKP and PKIKP, *Nature*, *356*, 309-314, 1992.

Creager, K.C., Inner core rotation rate from small-scale heterogeneity and time-varying travel times, *Science*, *278*, 1284-1288, 1997.

Creager, K.C., Large-scale variations in inner core anisotropy, In press in *J. Geophys. Res.*, 1999.

Durek, J. and B. Romanowicz, Inner core anisotropy inferred by direct inversion of normal mode spectra, In press *Geophys. J. Int.*, 1999.

He, X. and J. Tromp, Normal-mode constraints on the structure of the Earth, *J. Geophys. Res.*, *101*, 20,053-20,082, 1996.

Li, X-D., and B. Romanowicz, Global mantle shear velocity model developed using nonlinear asymptotic coupling theory, *J. Geophys. Res.*, *101*, 22,245-22,272, 1996.

Li, X-D., D. Giardini, and J. H. Woodhouse, Large-scale three-dimensional even-degree structure of the Earth from splitting of long-period normal modes, *J. Geophys. Res.*, *96*, 551-557, 1991.

Morelli, A., A.M. Dziewonski, and J. H. Woodhouse, Anisotropy of the core inferred from PKIKP travel times, *Geophys. Res. Lett.*, *13*, 1545-1548, 1986.

Morelli, A., A.M. Dziewonski, and J. H. Woodhouse, Anisotropy of the core inferred from PKIKP travel times,

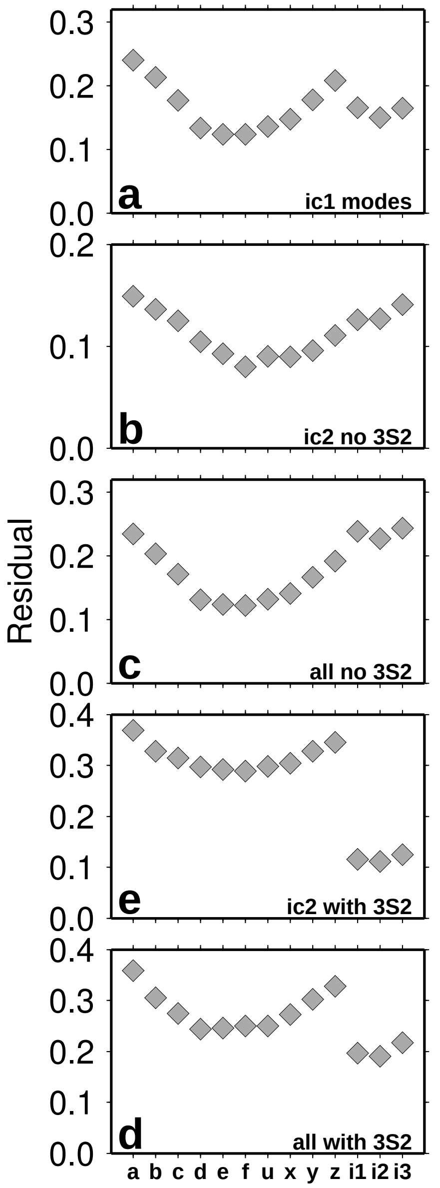

Figure 11.6: Residual variances for C20 as a function of model parametrization for the different subsets of data considered: (a) mantle, outer core and ic1 modes; (b) mantle, outer core and ic2 modes, without 3S2; (c) all modes without 3S2; (d) same as (b) with 3S2; (e) all modes with 3S2.

Geophys. Res. Lett., *13*, 1545-1548, 1986.

Poupinet, G., R. Pillet, and A. Souriau, Possible heterogeneity of the Earth's core deduced from PKIKP travel times, *Nature*, *305*, 204-206, 1983.

Ritzwoller, M., G. Masters, and F. Gilbert, Observations of anomalous splitting and their interpretation in terms of aspherical structure, *J. Geophys. Res.*, *91*, 10203-10228, 1988.

Romanowicz, B., X.-D. Li, and J. Durek, Anisotropy in the inner core; could it be due to low-order convection? *Science*, *274*, 963-966, 1996.

Shearer, P.M., PKP(BC) versus PKP(DF) differential travel times and aspherical structure in the Earth's inner core, *J. Geophys. Res.*, *96*, 2233-2247, 1991.

Song, X.-D. and D.V. Helmberger, Seismic evidence for an inner core transition zone, *Science*, *282*, 924-927, 1998.

Su, W. and A.M. Dziewonski, Inner core anisotropy in three dimensions. *J. Geophys. Res.*, *100*, 9831-9852, 1995.

Tanaka, S. and H. Hamaguchi, Degree one heterogeneity and hemispherical variation of anisotropy in the inner core from PKP(BC)-PKP(DF) times, *J. Geophys. Res.*, *102*, 2925-2938, 1997.

Tromp, J., Support for anisotropy of the Earth's inner core from splitting in free oscillation data, *Nature*, *366*, 678-681, 1993.

Vinnik, L., B. Romanowicz, and L. Bréger, Anisotropy in the central part of the inner core. *Geophys. Res. Lett.*, *21*, 1671, 1994.

Widmer, R., G. Masters, and F. Gilbert, Observably split multiplets-data analysis and interpretation in terms of large-scale aspherical structure, *Geophys. J. Int.*, *111*, 559-576, 1992.

Woodhouse, J.H., D. Giardini, and X.-D. Li, Evidence for inner core anisotropy from splitting in free oscillation data, *Geophys. Res. Lett.*, *13*, 1549-1552, 1986.

4. The 3D shear velocity structure of the mantle from the inversion of body, surface, and higher mode waveforms

Charles Mégnin & Barbara Romanowicz

4.1 Introduction

The last two decades have produced a large collection of tomographic models of the mantle on a global scale, with the scale length of the structure resolved increasing with time. Significant improvements to the quality of images of the deep mantle have been the result of efforts aimed at deriving a theoretical formalism for body waves as accurate and computationally efficient as possible. The emergence of time-domain waveform tomography suited to the modeling of body waves (*Li & Romanowicz*, 1995) has allowed to treat the data in a normal mode theoretical framework 'Nonlinear Asymptotic Coupling Theory' (NACT) that accommodates the existence of Fresnel zones, and allows the modeling of all the energy on the seismic trace, providing excellent sampling of mantle structure. A waveform extraction scheme in which each energy arrival in the seismic trace is selected separately has proved a powerful tool to resolve lowermost mantle structure (*Mégnin & Romanowicz*, 1999). A model of the shear velocity structure of the mantle expanded laterally up to spherical harmonic degree 12 and radially in Legendre polynomials was derived with this methodology from the inversion of transverse component waveforms of body and surface waves for events of magnitude greater than 5.5 for the period from 1977 to 1994 recorded at IRIS and GEOSCOPE stations (*Li & Romanowicz*, 1996). In the present study, we used the same methodology to derive a higher resolution model '*SAW24B16*' expanded laterally up to degree 24 and radially in cubic b-splines. The adoption of local basis functions in the radial parametrization allows to accommodate the varying ray sampling of mantle structure with depth, which is precluded by the use of global basis functions. Taking advantage of recent deployments of broadband seismograms, we expanded the existing collection of seismograms with new body and fundamental surface wave information, and introduced higher mode waveforms into the data set. The present model was derived from the inversion of 31,000 body waves, 9,300 fundamental and 1,400 overtone surface waves.

4.2 Results

4.2.1 Fast anomalies

Our model shows in general fast anomalies associated with subduction that agree with results from many regional studies. In figure 11.7, we show such an example for the West Pacific. The top of the figure shows the model at 175 km depth in that region. Fast anomalies are associated with the Australian and Asian continents. Slow anomalies offshore correlate with mid-ocean ridges as well as back-arc spreading.

Figure 11.7 (A) is a cross section of the model across the southern Kurile Islands region, displaying a subhorizontal slab sinking to the 670 km discontinuity without entering the lower mantle. This observation is consistent with V_p models derived from *ISC* data (*e.g. Fukao et al.*, 1992).

The cross-section of figure 11.7 (B) is taken across the Japan Trench. The slab appears to 'rest' horizontally on the discontinuity, in agreement with (*e.g. van der Hilst et al.*, 1991). The anomaly penetrates into the lower mantle at its eastern end. The amplitude of this feature is nevertheless weak and may not be well resolved but it agrees qualitatively with the results of *Tajima et al.*, 1998.

The cross-section of figure 11.7 (C) is taken across the Mariana trench region and suggests that slab structure is present in the lower mantle, down to a depth of about 900 km.

In the region across the Solomon trench (figure 11.7 (D)), the slab appears to be confined to the transition zone and the uppermost part of the lower mantle. In contrast, the section across the Tonga-Kermadec region suggests that the slab penetrates into the lower mantle (figure 11.7 (E)). Continuation of the Tonga slab into the lower mantle has been observed previously (*e.g. Fisher et al.*, 1991).

In figure 11.7 (F), we show a cross-section across the Java subduction zone. The image suggests the presence of slab in the deep mantle, in agreement with *Fukao et al.*, 1992. Although this figure suggests that the slab reaches the CMB, the amplitudes below 1,500 km are low, indicating that the depth extent of this fast anomaly may not be reliably addressed with the present model.